Proc. Natl. Acad. Sci. USA
Vol. 96, pp. 6382–6387, May 1999
Medical Sciences

p27 and Rb are on overlapping pathways suppressing tumorigenesis in mice

MICHELE S. PARK*†, JUAN ROSAI‡, HAI T. NGUYEN†, PAOLA CAPODIECI‡, CARLOS CORDON-CARDO‡, AND ANDREW KOFF*†§

*Program in Molecular Biology and ‡Department of Pathology, Memorial Sloan–Kettering Cancer Center, 1275 York Avenue, New York, NY 10021; and †Cornell University Graduate School of Medical Sciences, 1300 York Avenue, New York, NY 10021

Edited by George F. Vande Woude, National Institutes of Health, Frederick, MD, and approved March 25, 1999 (received for review October 15, 1998)

ABSTRACT **The commitment of cells to replicate and divide correlates with the activation of cyclin-dependent kinases and the inactivation of Rb, the product of the retinoblastoma tumor suppressor gene. Rb is a target of the cyclin-dependent kinases and, when phosphorylated, is inactivated. Biochemical studies exploring the nature of the relationship between cyclin-dependent kinase inhibitors and Rb have supported the hypothesis that these proteins are on a linear pathway regulating commitment. We have been able to study this relationship by genetic means by examining the phenotype of *Rb*+/−*p27*−/− mice. Tumors arise from the intermediate lobe cells of the pituitary gland in *p27*−/− mice, as well as in *Rb*+/− mice after loss of the remaining wild-type allele of Rb. Using these mouse models, we examined the genetic interaction between Rb and p27. We found that the development of pituitary tumors in *Rb*+/− mice correlated with a reduction in p27 mRNA and protein expression. To determine whether the loss of p27 was an indirect consequence of tumor formation or a contributing factor to the development of this tumor, we analyzed the phenotype of *Rb*+/−*p27*−/− mice. We found that these mice developed pituitary adenocarcinoma with loss of the remaining wild-type allele of Rb and a high-grade thyroid C cell carcinoma that was more aggressive than the disease in either *Rb*+/− or *p27*−/− mice. Importantly, we detected both pituitary and thyroid tumors earlier in the *Rb*+/−*p27*−/− mice. We therefore propose that Rb and p27 cooperate to suppress tumor development by integrating different regulatory signals.**

A number of proteins prevent entry of cells into S phase. One group, Rb and the related proteins p107 and p130, act by redirecting or sequestering transcription factors regulating genes required for S phase (1, 2). Another group, members of the Ink4 (p15, p16, p18, and p19) and Cip/Kip families (p21, p27, and p57), act by inhibiting the cyclin-dependent kinases (cdks), CDK4/6 and CDK2 (3). Furthermore, these kinases are responsible for the coordinate phosphorylation and inactivation of the growth-suppressive functions of Rb (4–6). In tumor-derived cell lines lacking Rb, CDK4 function is dispensable for entry into S phase (7). However, CDK2 kinase activity is essential for proliferation, irrespective of Rb status, suggesting that, in addition to its role in inactivation of Rb, CDK2 has another function required for S phase (8).

These cell-culture-based studies suggest that CDK4 and Rb lie in a common regulatory pathway, whereas CDK2 regulates Rb inactivation and an as-yet unidentified pathway. Biochemical studies on the association of p27 with cyclin D2/CDK4 and cyclin E/CDK2 complexes have shown that, at physiological amounts, p27 seems to inhibit CDK2 preferentially over CDK4 (9, 10). Based on these studies, we speculated that the simultaneous disruption of p27 and Rb might mimic the constitutive activation of the CDK2 pathway and remove the requirement for the CDK4 pathway. A caveat, however, is that the relationship between these proteins was established in immortalized and transformed cell lines, and any effect of immortalization or culture conditions would have been obscured. Thus, we wanted to determine the nature of the relationship between Rb and p27 in a normal biologic context—a mouse model system.

Mice harboring mutations of each member of the Rb and Cip/Kip families have been generated. *Rb*−/− mice die during embryogenesis (11–13), and thus we cannot study the effect of this mutation in every tissue. However, after loss of heterozygosity (LOH) at the Rb locus, *Rb*+/− mice develop melanotroph tumors that contain cells that are effectively *Rb*−/− (12–15). Tumor development in *Rb*+/− mice is observed only after a long latency period after the loss of the wild-type allele (15). LOH occurs within the first 60 days after birth in 72% of the mice, and by day 90, 94% of the mice have undergone at least one LOH event. After LOH, *Rb*−/− melanotrophs continue to proliferate; however, when these cells are innervated by the dopaminergic (D2) neuron, they undergo apoptosis (15). It is only after another "hit," which makes the cells refractory to the growth-suppressive signals from the D2 neuron, that the tumor begins to develop. Extraordinarily, *p27*−/− mice also develop melanotroph tumors (16–18). Hyperplasia of p27-deficient pituitary glands is observed as early as 11 weeks of age (16–18). Melanotrophs express both Rb (15) and p27, suggesting that these proteins regulate melanotroph proliferation in a cell-autonomous manner. Thus, studying tumor development in this system will allow us to determine whether Rb and p27 are linked in a common pathway.

We intercrossed *Rb*+/− and *p27*−/− mice to generate *Rb*+/−*p27*−/− mice to understand better the interactions between these proteins in an otherwise "normal" genetic background. We found that development of pituitary tumors in *Rb*+/− mice correlated with a reduction in p27 mRNA and protein expression. To determine whether this observed reduction of p27 was causal or consequential to tumor development, we asked whether the loss of p27 would accelerate the development of tumors in *Rb*+/− mice. We found that in a *p27*-deficient background, LOH at the *Rb* locus led to a significantly earlier appearance of pituitary adenocarcinoma. Additionally, we have shown that *Rb*+/− and *p27*−/− mice develop thyroid C cell carcinoma. In *Rb*+/−*p27*−/− mice, these tumors are more aggressive and are detectable earlier. Thus, we conclude that the absence of p27 enhances the

The publication costs of this article were defrayed in part by page charge payment. This article must therefore be hereby marked "*advertisement*" in accordance with 18 U.S.C. §1734 solely to indicate this fact.

PNAS is available online at www.pnas.org.

This paper was submitted directly (Track II) to the *Proceedings* office.
Abbreviations: cdk, cyclin-dependent kinase; D2, dopaminergic; LOH, loss of heterozygosity; EAP, early atypical proliferate.
§To whom reprint requests should be addressed. e-mail: a-koff@ski.mskcc.org.

tumorigenic phenotype in Rb+/− mice, suggesting that the loss of p27 is causal for tumor development. This conclusion suggests that Rb and p27 act cooperatively to affect tumor development.

MATERIALS AND METHODS

Genotyping of Animals. Animals were genotyped for Rb from tail DNA by using three-primer PCR as described (13). Genotyping for p27 was performed by immunoblotting blood samples with a 1:3,000 dilution of affinity-purified p27 antibody to detect the wild-type band migrating at 27 kDa and the truncated mutant band migrating at 21 kDa.

Histological Analysis. Tissues were surgically removed, fixed in 10% buffered formalin overnight, embedded in paraffin, sectioned at 5–7 μm, and stained with hematoxylin and eosin before microscopic analysis. All magnifications in legends represent objective lens.

Immunohistochemistry. Immunohistochemical detection of p27 protein and Ki67 nuclear antigen was performed on 7-μm-thick paraffin sections of formalin-fixed samples with the use of avidin/biotin/peroxidase detection (Elite Vectastain ABC kit from Vector Laboratories). To facilitate antigen recognition by the antibodies, slides were microwaved in 0.01 M citric acid for 10 min and then quenched in 1% H_2O_2 for 10 min. Slides were incubated subsequently in 10% normal goat-serum diluted in 4% BSA/PBS to block nonspecific interactions. Primary antibodies were used as follows: p27 was detected with an affinity-purified rabbit polyclonal antibody raised against a glutathione *S*-transferase full-length murine p27 fusion protein. This antibody was purified as described (19) and used at a 1:30,000 dilution in 4% (vol/vol) BSA/PBS. For the antigen blocking experiment, this antibody was incubated overnight with 10 μg of His–p27 before application to the slide. Ki67 was detected by using NCl–Ki67p (NovoCastra, Newcastle, U.K.) at a 1:10,000 dilution in 4% (vol/vol) BSA/PBS. The secondary antibody (goat anti-rabbit biotinylated IgG) was used at a 1:1,000 dilution.

Detection of chromogranin and thyroglobulin was performed on similarly fixed, mounted, and microwaved sections; however, blocking was performed with normal horse or normal goat serum [1:40 dilution in 2% (vol/vol) BSA/PBS], respectively. A mouse monoclonal antibody to chromogranin (Boehringer Mannheim) was used at a 1:5,000 dilution. A rabbit polyclonal antibody to thyroglobulin (Dako A251) was used at a 1:100,000 dilution. We used biotinylated secondary antibodies (Vector Laboratories) and peroxidase-conjugated streptavidin to allow detection by diaminobenzidine.

***In Situ* Hybridization.** Antisense [^{33}P]UTP-labeled p27-specific riboprobes were generated by linearizing pSKp27 with *Xba*I and transcribing with T7 polymerase. Control sense probes were generated by linearizing with *Xho*I and transcribing with T3 polymerase. *In situ* hybridization was performed as described (20). Briefly, one set of two slides was processed for autoradiography by using Kodak emulsion NTB-2 and exposed on day 4—the other on day 7. Silver grains were counted by using Nomarski optics on a Zeiss Axiophot microscope with oil immersion at a ×100 magnification. Values for the number of black grains detected per cell were obtained in 5–8 random fields of view per section in a total of two to six sections for *Rb*+/− and wild-type pituitaries. This analysis was repeated three times with samples from different mice each time as well as a new preparation of probe. Very little variance in the trend of the distribution was observed, although the range of grains per cell varied as a reflection of labeling efficiency.

Southern Analysis of Tumor DNA. Tumor samples were surgically removed, and DNA was prepared as described (21). For determination of *Rb* status, tumor DNA was digested with *Pst*I and hybridized with a probe derived from the second intron of the *Rb* gene (13).

RESULTS AND DISCUSSION

p27 Expression Is Reduced in Pituitary Tumors Arising in *Rb*+/− Mice. Mice with a heterozygous mutation at the *Rb* locus as well as mice deficient for p27 have abnormal growth in the melanotroph cells of the pituitary. To determine whether p27 might be involved in the development of pituitary adenocarcinoma in *Rb* mutant mice, we examined the expression of p27 protein and RNA in tumors isolated at autopsy. In wild-type mice, staining for p27 was more intense in pituitary cells than in adjacent brain tissue (Fig. 1 *a* and *b*). Antibody reactivity was blocked completely by addition of antigen (Fig. 1*c*), and tissue was not stained if the primary antibody was omitted (Fig. 1*d*). In contrast, in pituitary tumors of *Rb*+/− mice, even when the detection reaction was allowed to proceed until the adjacent brain tissue was positive (Fig. 1*f*), there was negligible staining for p27 in the tumor cells (Fig. 1*e*).

p27 is the target of multiple regulatory inputs, including S phase-specific proteolysis (22, 23), G_0-specific translational controls (24–26), and transcription (27, 28). To determine which might account for the loss of p27 in the tumors, we examined expression of p27 mRNA. The expression of S26 mRNA, a nonspecific message encoding a ribosomal subunit (29), was equivalent in tissue obtained from wild-type mice and in tumors obtained from *Rb*+/− mice. In contrast, the expression of p27 mRNA was reduced ≈2- to 3-fold in tumor cells compared with wild-type cells of the pituitary. It was therefore apparent that the p27 message was down-regulated, but not ablated completely, during tumor development (Fig.

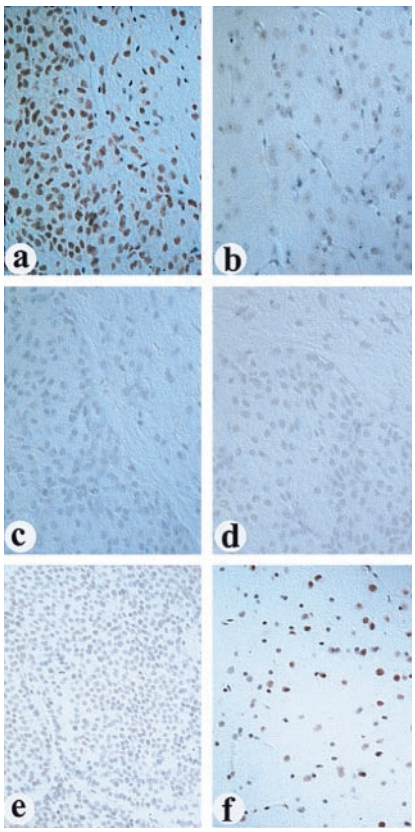

FIG. 1. p27 protein expression is reduced in pituitary tumors arising in *Rb* heterozygous mice. The specificity of the p27 antibody was determined by comparing the reactivity in wild-type pituitary cells (*a*) and wild-type adjacent brain tissue (*b*). Pituitary reactivity could be blocked by inclusion of excess antigen (*c*) or exclusion of primary antibody (*d*). Note the staining of p27 is greater in the pituitary cells than in the adjacent brain cells. A reciprocal pattern of accumulation is observed when comparing the pituitary tumor (*e*) and normal brain tissue (*f*) obtained from *Rb*+/− mice. (Magnification: ×40.)

2). This result indicated that Rb might participate in the regulation of p27 mRNA, at least in intermediate lobe melanotrophs, and raised the possibility that the loss of p27 was a consequence of tumor development and not related causally to tumor development.

Decreased Viability but Similar Tumor Types Are Observed in *Rb+/−p27−/−* Mice. *p27−/−* mice develop a benign hyperplastic lesion, and *Rb+/−* mice develop a more aggressive pituitary adenocarcinoma. The significant difference in the nature of these tumors suggested that if the loss of p27 was a consequence of the loss of Rb in tumors, Rb might be regulating other events in addition to its regulation of p27 mRNA. Thus, we predicted that if the loss of p27 was involved in development of tumors in *Rb+/−* mice, then mice with the *Rb+/−p27−/−* genotype would experience greatly accelerated tumor formation, and these tumors would resemble morphologically the tumors developing in *Rb+/−* mice. However, if the loss of p27 was simply a consequence of tumor development in *Rb+/−* mice, then the tumor phenotypes would be comparable with respect to onset and morphology. To test these predictions, we mated females heterozygous for the Rb^{x3t} allele (13) with males homozygous for the $p27^{D51}$ allele (18) to generate animals heterozygous for both mutations. These mice were intercrossed to generate animals heterozygous for the *Rb* mutation and homozygous for the *p27* mutation.

The mean age of death for *Rb+/−p27+/−* mice was reduced slightly compared with animals heterozygous for the *Rb* mutation alone (Fig. 3). The mean age at death of *Rb+/−p27+/−* mice was 280 days, with ages ranging from 169 days to 378 days. The mean age at death of *Rb+/−* mice was 337 days, with ages ranging from 251 days to 406 days. In contrast, the mean age of death for *Rb+/−p27−/−* mice was significantly lower than *Rb+/−* or *p27−/−* animals, with the mean age at death being 178 days with a range of 118–217 days.

We next determined the spectrum of tumors in *Rb+/−p27+/+*, *Rb+/−p27+/−*, and *Rb+/−p27−/−* mice at autopsy (Table 1). We readily detected pituitary hyperplasia/adenoma and a low grade C cell carcinoma in *p27−/−* mice. *Rb*-mutant mice developed pituitary adenocarcinoma and thyroid C cell carcinoma. *Rb+/−p27+/−* and *Rb+/−p27−/−* mice developed the same spectrum of tumors observed in *Rb+/−p27+/+* mice.

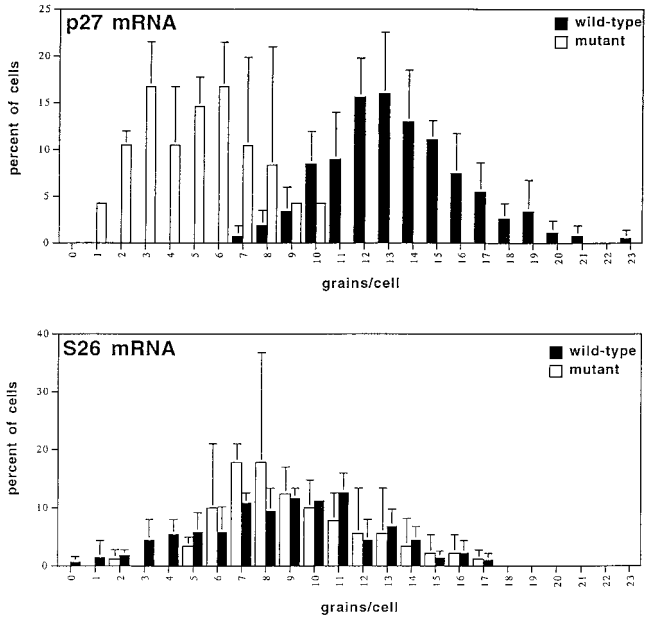

FIG. 2. p27 mRNA expression is reduced in pituitary tumors arising in *Rb* heterozygous mice. The percentage of cells with a particular number of grains is plotted on the ordinate. The data from a representative experiment are shown. (*Top*) The distribution of p27 mRNA. (*Bottom*) The distribution of S26 mRNA (a nonspecific control). Wild-type tissue is represented by black bars, and tumor tissue is represented by the white bars.

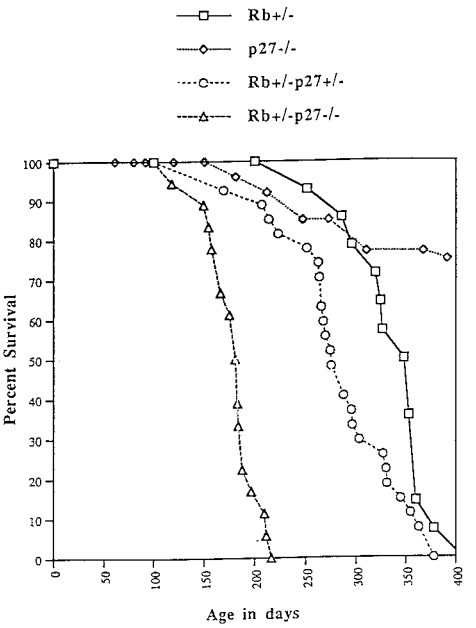

FIG. 3. Survival of mice with mutations in *Rb* and *p27*. The graph summarizes the viability of mice for each genotype ($n = 30$, *p27−/−*; $n = 10$, *Rb+/−*; $n = 20$, *Rb+/−p27+/−*; $n = 30$, *Rb+/−p27−/−*). The mean age of survival is given in *Results and Discussion*.

Pituitary Tumorigenesis in *Rb+/−p27−/−* Mice. All 22 *Rb+/−p27−/−* animals developed adenocarcinoma of the pituitary, similar to the conditions observed in the *Rb+/−p27+/+* animals. However, the tumors in the *Rb+/−p27−/−* mice were more aggressive and displayed more severe features: hemorrhaging, necrosis, and invasion into adjacent brain structures (Fig. 4). These tumors sustained the loss of the remaining wild-type allele of *Rb* (Fig. 4).

We noted variability in the size of cells and the intensity of hematoxylin in 4 of 13 tumors isolated from *Rb+/−p27−/−* mice at autopsy. We did not observe similar variability in any of the tissues or tumors obtained from wild-type, *p27*-deficient, or *Rb*-mutant mice (Fig. 4). In these four tumors, we identified three types of cells: a small cell with highly condensed nuclei, and medium and large cells with less intense nuclear staining (Fig. 4 *d–f*). We observed the small-cell phenotype only in the largest tumors (Fig. 4*g*). The remaining tumors clustered at sizes similar to those observed in *Rb+/−p27+/+* mice (5 ± 0.7 mm; mean ± SD; $n = 6$).

This cell type and its presence in only the largest tumors was intriguing. The characteristics of this cell, small with dense-staining nuclei, were reminiscent of senescent cells found in many human tumors. To determine whether this cell type was proliferating, we asked whether it was reactive to Ki67 anti-

Table 1. Incidence of pathological lesions in mice with *Rb* and *p27* mutations at autopsy

Lesion	*p27−/−* 7–15 mos	*Rb+/−* 10–12 mos	*Rb+/− p27+/−* 7–15 mos	*Rb+/− p27−/−* 5–7 mos
Pituitary adenoma	7/10	0/5	0/10	0/22
Pituitary carcinoma	0/10	4/5	7/10	19/22
Thyroid C cell carcinoma	3/10	3/5	8/10	17/22

Pathology was noted by gross and microscopic evaluations at the time of death or sacrifice because of morbidity.

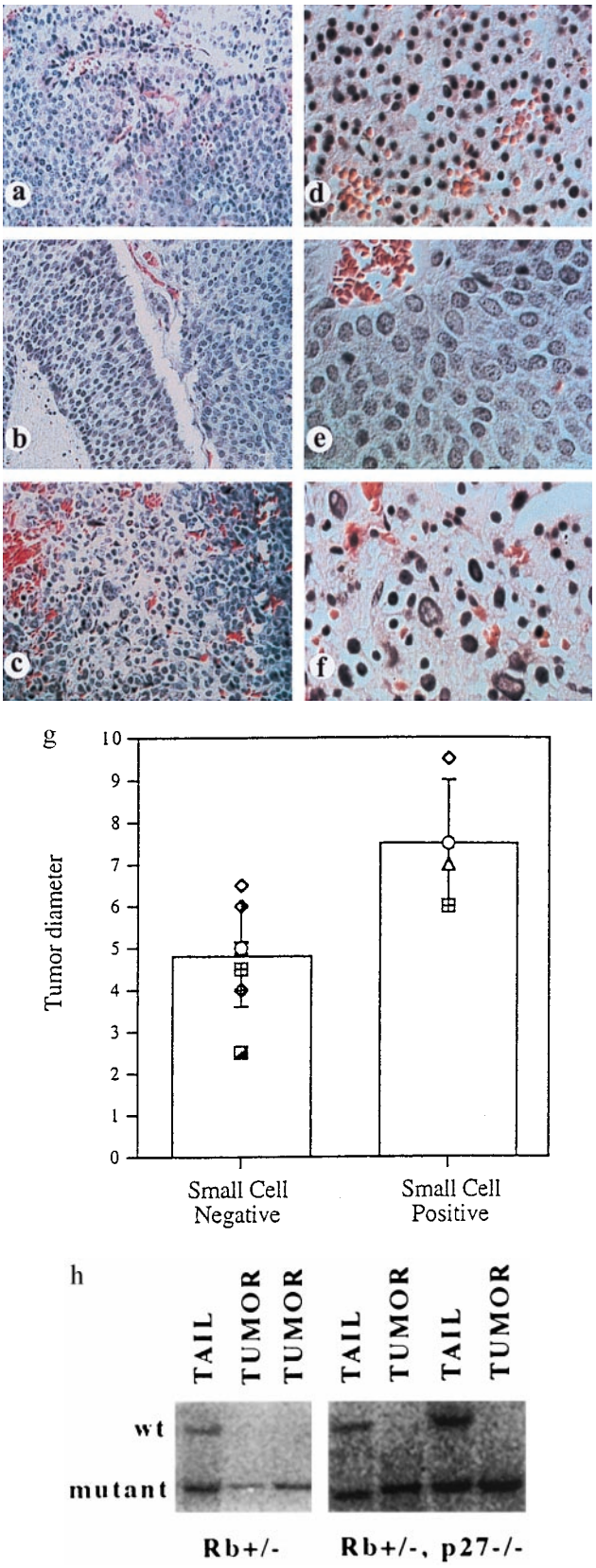

FIG. 4. Pituitary tumorigenesis. (*a–c*) Representative sections through *Rb*+/−, *p27*−/−, and *Rb*+/−*p27*−/− tissues and tumors are shown at ×40 magnification. (*d–f*) Higher magnification (×100) of the different cell types observed in the *Rb*+/−*p27*−/− tumor. (*g*) Small-cell phenotype correlates with the largest tumor volumes. The tumor volume is plotted on the ordinate and is shown as a function of the absence (left bar) or presence (right bar) of the small-cell-morphology phenotype. The bars represent the mean, and the SD is included for the samples, each indicated by a character. (*h*) *Rb* genotype in the pituitary tumors. The loss of Rb was determined by Southern blotting DNA prepared from two tissues of either *Rb*+/− or *Rb*+/−*p27*−/− animals. As a control for the wild-type (wt) allele, tail DNA obtained from the animal was processed similarly. The source of tissue is indicated above each lane. The genotype of the animal is below each panel, and the migration of the Rb allele is on the left. We used only tail DNA from an *Rb*+/− animal.

Table 2. Onset of pituitary adenocarcinoma

Phenotype	Time of sacrifice, weeks		
	10	15	20–28
Rb+/−*p27*+/+	0/5	0/12	3/15
Rb+/−*p27*−/−	2/3	8/10	19/22

Pathology was noted by gross examination of the pituitary at the time of sacrifice indicated.

body, a marker often used to identify proliferating cells in tissue sections. These small cells were negative; of 1,200 cells examined, only 9 were positive (average of 0.3 positive cells per field of view with only nine fields having a positive cell). In contrast, 8.1% and 9.2% of medium cells, in small-cell-positive and small-cell-negative tumors, respectively, stained with Ki67 antibody. In both cases, the range was 0–18% in each field analyzed with only a few completely negative fields. This value was comparable to that observed in tumors obtained from *Rb*+/− mice (10% positive with values ranging from 2% to 18% for each field of view). Only 8 of 689 wild-type intermediate lobe cells (≈1.2%) were positive for Ki67. This result is consistent with the hypothesis that the small cells were nonproliferative and perhaps senescent. These cells were not apoptotic, as determined by terminal deoxynucleotidyltransferase-mediated UTP-labeling assay (data not shown).

The age discrepancy at the times of death of *Rb*+/−*p27*−/− and *Rb*+/−*p27*+/+ mice prompted us to determine the time at which pituitary abnormalities could be detected in these two strains of mice (Table 2). In wild-type mice, melanotroph proliferation normally ceases between postnatal day 35 and 60 (15). However, in *Rb*+/− mice, small morphologically distinct clusters of proliferating cells (EAPs, early atypical proliferates) continue to be observed; by postnatal day 90, ≈94% of mice have at least one of these EAPS (15). It is important to note that the latency between EAP formation and tumor development might be attributed to apoptosis induced in *Rb*−/− cells when innervated by the D2 neuron (15). Thus, we reasoned that if loss of p27 were involved in the tumorigenic process, then we would detect tumors earlier in *Rb*+/−*p27*−/− mice compared with *Rb*+/−*p27*+/+ mice. As shown in Table 2, we readily observed tumors in two of three *Rb*+/−*p27*−/− animals as early as 10 weeks of age but in none of the five in *Rb*+/−*p27*+/+ animals. These differences were maintained throughout 15 weeks and 20–28 weeks, by which time, all *Rb*+/−*p27*−/− animals died. The earlier detection of abnormal growth in the pituitaries of *Rb*+/−*p27*−/− animals suggested that tumors either arose earlier or progressed faster in the background of a p27 deficiency.

Summarizing the data presented here and those presented by others yields the following conclusions regarding melanotroph tumor development in *Rb*+/− mice. First, EAPs form early in mouse development; however, because cells undergo apoptosis when innervated by the D2 neuron, a tumor cannot develop until those cells become refractory to that signal. Thus, after LOH at the *Rb* locus, tumor development depends on a cell either losing the ability to respond to D2 signals or acquiring resistance to apoptosis induced by D2 signaling. Second, *p27*−/− mice develop pituitary hyperplasia, a finding consistent with an inability of these cells to respond appropri-

ately to the antimitogenic influences of the D2 neuron. We have shown that this antimitogenic function of p27 regulates the growth and differentiation properties of oligodendrocytes (30, 31) and the growth properties of luteal cells (32). Thus, we speculate that the earlier appearance of tumors in the *Rb+/−p27−/−* mice was caused by a loss of D2-neuron-induced cell death after LOH at the Rb locus. The appearance of small senescent-like cells in a subset of tumors might be a consequence of the time at which the LOH event occurred. The earlier in the 90-day window, the more likely the tumor was to reach its Hayflick limit.

This model, like all incipient models, requires further testing. Much of that will require the ability to score EAPs, which is not possible currently with our limited expertise in pathological scoring of this lesion. However, the model also relies on establishing the growth and transformation properties of cells lacking Rb and p27. These can be addressed by studying the growth and differentiation properties of mouse embryonic fibroblasts.

Thyroid Tumorigenesis in *Rb+/−p27−/−* Mice. In addition to the pituitary tumor readily observed on gross pathological analysis, we also observed a high frequency of thyroid disease observable in microscopic analysis in the *p27−/−*, *Rb+/−*, and *Rb+/−p27−/−* animals. Normally, thyroid tissues contain large follicles surrounded by follicular cells (thyroglobulin-positive) and scattered C cells (chromagranin-positive; Fig. 5*A*). Cross-sectional analysis allows detection of two lobes separated by the trachea. In *p27−/−* and *Rb+/−* mice, there was an obvious unilateral expansion of cells (Fig. 5*B*). These tumors stained diffusely or focally for chromogranin, suggesting that they originated in the C cells (data not shown). Generally, these tumors were small (p27−/−, $n = 3$; Rb+/−, $n = 5$), were confined to one lobe, and were not noted on gross examination as they did not alter the gross appearance of the thyroid. However, in one *Rb+/−* mouse, the tumor was bilateral, had a region of necrosis, and did alter the gross appearance of the thyroid.

In *Rb+/−p27−/−* mice, these tumors were larger, allowing obvious detection during gross analysis (13/15), and often

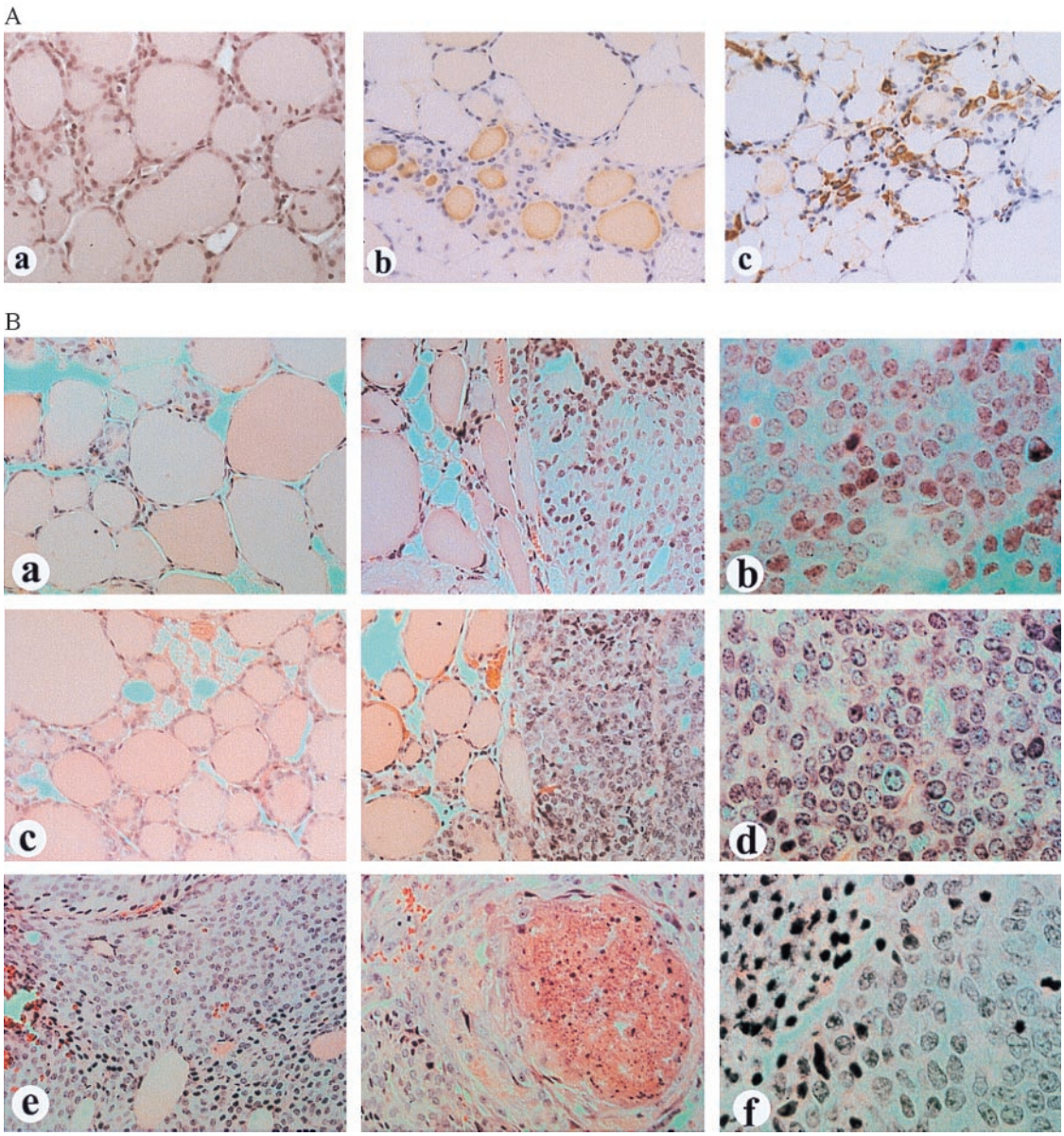

FIG. 5. Thyroid tumorigenesis. (*A*) Morphologic and immunohistochemical features of the thyroid. Hematoxylin and eosin staining (*a*) shows the presence of large follicles surrounded by C cells (chromogranin-positive cells in *c*) and thyroglobulin-producing cells (*b*). (Magnification: ×40.) (*B*) Representative sections through *Rb+/−* (*a* and *b*), *p27−/−* (*c* and *d*), and *Rb+/−p27−/−* (*e* and *f*). (*a*, *c*, and *e*, magnification: ×40. *b*, *d*, and *f*, magnification: ×100.) *a, c,* and *e* represent the two lobes of the thyroid.

Table 3. Onset of thyroid C cell carcinoma

Phenotype	Time of sacrifice, weeks 15	20–28
Rb+/−p27+/+	0/6	1/15
Rb+/−p27−/−	3/6	17/22

Pathology was noted by microscopic evaluation of the thyroid at the time of sacrifice indicated.

bilateral (12/15); necrosis was readily apparent (8/15). There was no correlation between necrosis and a tumor being bilateral, because one of the three unilateral tumors had a necrotic region. Overall, these tumors display some features suggesting a greater malignancy than *Rb+/−* or *p27−/−* tumors, including a few tripolar mitotic figures (data not shown) and a less differentiated phenotype. Additionally, we noted that the onset of thyroid tumors also was accelerated by the p27 deficiency (Table 3). These data suggested that Rb and p27 cooperated in the development of C cell carcinoma.

CONCLUSION

The data presented here—(*i*) loss of p27 during development of pituitary adenocarcinoma in *Rb*-mutant mice, (*ii*) the early onset of pituitary tumors in *Rb+/−p27−/−* mice, (*iii*) LOH at the *Rb* locus in double-mutant pituitary tumors, (*iv*) the identification of an altered morphology in a subset of pituitary tumors, and (*v*) similar observations for the thyroid tumors—argue for a cooperative relationship between p27 and Rb in the suppression of tumorigenesis in mice. Nevertheless, they do not eliminate the possibility that these proteins may be on a common pathway. For example, these proteins are both inactivated by cyclin D/CDK complexes. Cyclin D/CDK complexes can sequester p27 (9, 10, 33) and prevent it from inhibiting cyclin E/CDK2. They can also phosphorylate Rb, inactivating its ability to interact with E2F (34–36). Therefore, the activation of cyclin D1/CDK4 complexes may alleviate two growth suppressive mechanisms to facilitate tumor development. Because ras regulates MEK1, which is involved in the activation of cyclin D1/CDK4 complexes (37), it is tempting to speculate that primary cells deficient in both Rb and p27 might act like ras-transformed cells. Continuing work on embryonic fibroblasts is necessary to address this model of cooperativity.

The authors thank Tyler Jacks (Massachusetts Institute of Technology, Cambridge, MA) for making the *Rb+/−* mice available to us, Bruce Stillman and Moshe Oren for comments on the work as it was developing, Mary Baylies and Tyler Jacks for critically evaluating the manuscript, and Stacy Blain, Antonio Iavarone, and Beverly Warner for suggestions throughout the course of this work. This work was supported by the Memorial Sloan–Kettering Cancer Center/National Cancer Institute Core Grant CA08748 to A.K., by the National Cancer Institute's SPORE program Grant CA68425, and by the Koch fund of CAPcure. A.K. is a Pew Scholar in Biomedical Science, an Irma T. Hirschl Scholar, and the incumbent of the Frederick R. Adler Chair for Junior Faculty at the Memorial Sloan–Kettering Cancer Center.

1. Dyson, N. (1998) *Genes Dev.* **12,** 2245–2262.
2. Nevins, J. R. (1998) *Cell Growth Differ.* **9,** 585–593.
3. Sheaff, R. J. & Roberts, J. M. (1998) in *Cell Cycle Control*, ed. Pagano, M. (Springer, New York), pp.1–34.
4. Kitagawa, M., Higashi, H., Jung, H. K., Takahasi, K., Suzuki, I., Ikeda, M., Tamai, K., Kato, J., Segawa, K., Yoshida, E., Nishimura, S., *et al*. (1996) *EMBO J.* **15,** 7060–7069.
5. Zarkowska, T. & Mittnacht, S. (1997) *J. Biol. Chem.* **272,** 12738–12746.
6. Lundberg, A. & Weinberg, R. A. (1998) *Mol. Cell. Biol.* **18,** 753–761.
7. Lukas, J., Bartkova, J., Rhode, M., Strauss, M. & Bartek, J. (1995) *Mol. Cell. Biol.* **15,** 2600–2611.
8. Ohtsubo, M., Theodoras, A. M., Schumacher, J., Roberts, J. M. & Pagano, M. (1995) *Mol. Cell. Biol.* **15,** 2612–2624.
9. Soos, T. J., Kiyokawa, H., Yan, J. S., Rubin, M. S., Giordano, A., DeBlasio, A., Bottega, S., Wong, B., Mendelsohn, J. & Koff, A. (1996) *Cell Growth Differ.* **7,** 135–146.
10. Blain, S. W., Montalvo, E. & Massagué, J. (1997) *J. Biol. Chem.* **272,** 25863–25872.
11. Clarke, A. R., Maandag, E. R., van Roon, M., van der Valk, N. M. T., Hooper, M. L., Berns, A. & te Reile, H. (1992) *Nature (London)* **359,** 328–330.
12. Lee, E. Y.-H. P., Chang, C. Y., Hu, N., Yang, Y. C., Lai, C. C., Herrup, K., Lee, W.-H. & Bradley, A. (1992) *Nature (London)* **359**, 288–294.
13. Jacks, T., Faxeli, A., Schmitt, E. M., Bronson, R. T., Goodell, M. A. & Weinberg, R. A. (1992) *Nature (London)* **359,** 295–300.
14. Hu, N., Gutsmann, A., Herbert, D. C., Bradley, A., Lee, W.-H. & Lee, E. Y.-H. P. (1994) *Oncogene* **9**, 1021–1027.
15. Nikitin, A. Y. & Lee, W.-H. (1996) *Genes Dev.* **10,** 1870–1879.
16. Fero, M. I., Rivkin, M., Tasch, M., Porter, P., Carow, C. E., Firpo, E., Polyak, K., Tsai, L.-H., Broudy, V., Perlmutter, R. M., et al. (1996) *Cell* **85**, 733–744.
17. Nakayama, K., Ishida, N., Shirane, M., Inomata, A., Inoue, T., Shishido, N., Horii, I., Loh, D. Y. & Nakayama, K. I. (1996) *Cell* **85**, 707–720.
18. Kiyokawa, H., Kineman, R. D., Manova-Todorova, K. O., Soares, V. C., Hoffman, E., Ono, M., Khanam, D., Hayday, A. C., Frohman, L. A. & Koff, A. (1996) *Cell* **85,** 721–732.
19. Koff, A., Cross, F., Fisher, A., Schumacher, J., Leguellec, K., Philippe, M. & Roberts, J. M. (1991) *Cell* **66,** 1217–1228.
20. Manova, K., Nocka, K., Besmer, P. & Bachvarova, R. F. (1990) *Development (Cambridge, U.K.)* **110,** 1057–1069.
21. Goelz, S. E., Hamilton, S. R. & Vogelstein, B. (1985) *Biochem. Biophys. Res. Commun.* **130,** 118–126.
22. Pagano, M., Tam, S. W., Theodoras, A. M., Beer-Romero, P., Del Sal, G., Chau, V., Yew, P. R., Draetta, G. F. & Rolfe, M. (1995) *Science* **269,** 682–685.
23. Nguyen, H., Gitig, D. M. & Koff, A. (1999) *Mol. Cell. Biol.* **19,** 1190–1201.
24. Hengst, L. & Reed, S. I. (1996) *Science* **271,** 1861–1864.
25. Agrawal, D., Hauser, P., McPherson, F., Dong, F., Garcia, A. & Pledger, D. W. (1996) *Mol. Cell. Biol.* **16,** 4327–4336.
26. Millard, S. S., Yan, J. S., Nguyen, H., Pagano, M., Kiyokawa, H. & Koff A. (1997) *J. Biol. Chem.* **272,** 7093–7098.
27. Verlinden, L., Verstuyf, A., Convents, R., Marcelis, S., Van Camp, M. & Bouillon, R. (1998) *Mol. Cell. Endocrinol.* **142,** 57–65.
28. Johnson, D., Frame, M. C. & Wyke, J. A. (1998) *Oncogene* **16,** 2017–2028.
29. Vincent, S., Marty, L. & Fort, P. (1993) *Nucleic Acids Res.* **21,** 1498.
30. Casaccia-Bonnefil, P., Tikoo, R., Kiyokawa, H., Friedrich, V., Chao, M. V. & Koff, A. (1997) *Genes Dev.* **11,** 2335–2346.
31. Durand, B., Fero, M. L., Roberts, J. M. & Raff, M. C. (1998) *Curr. Biol.* **8,** 431–440.
32. Tong, W., Kiyokawa, H., Soos, T. J., Park, M. S., Soares, V. C., Manova, K., Pollard, J. W. & Koff, A. (1998) *Cell Growth Differ.* **9,** 787–794.
33. Polyak, K., Kato, J., Solomon, M. J., Sherr, C. J., Massague, J., Roberts, J. M. & Koff, A. (1994) *Genes Dev.* **8**, 9–22.
34. Hatekeyama, H. & Weinberg, R. A. (1995) in *Progress in Cell Cycle Research*, eds. Meijier, L., Guidet, S. & Tung, H. Y. L. (Plenum, New York), pp. 9–19.
35. Weinberg, R. A. (1995) *Cell* **81,** 323–330.
36. Sherr, C. J. (1996) *Science* **274,** 1672–1677.
37. Cheng, M., Sexl, V., Sherr, C. J. & Roussel, M. F. (1998) *Proc. Natl. Acad. Sci. USA* **95,** 1091–1096.